

CrystEngComm

Accepted Manuscript



This is an *Accepted Manuscript*, which has been through the Royal Society of Chemistry peer review process and has been accepted for publication.

Accepted Manuscripts are published online shortly after acceptance, before technical editing, formatting and proof reading. Using this free service, authors can make their results available to the community, in citable form, before we publish the edited article. We will replace this *Accepted Manuscript* with the edited and formatted *Advance Article* as soon as it is available.

You can find more information about *Accepted Manuscripts* in the [Information for Authors](#).

Please note that technical editing may introduce minor changes to the text and/or graphics, which may alter content. The journal's standard [Terms & Conditions](#) and the [Ethical guidelines](#) still apply. In no event shall the Royal Society of Chemistry be held responsible for any errors or omissions in this *Accepted Manuscript* or any consequences arising from the use of any information it contains.

ARTICLE

The Diversity of Zn(II) Coordination Networks Composed of Multi-Interactive Ligand TPHAP^- via Weak Intermolecular Interaction

Cite this: DOI: 10.1039/x0xx00000x

Received 00th January 2012,
Accepted 00th January 2012

DOI: 10.1039/x0xx00000x

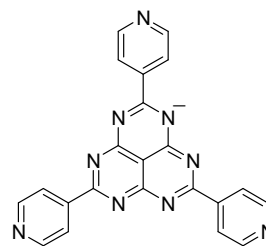
www.rsc.org/

Tatsuhiro Kojima,^a Tomofumi Yamada,^b Yumi Yakiyama,^a Eri Ishikawa,^c Yasushi Morita,^d Masahiro Ebihara,^b and Masaki Kawano^{*a}

Kinetic state networks can be trapped by multi-interactive ligands via weak intermolecular interactions. Self-assembly of a tripyridyl multi-interactive ligand K^+TPHAP^- (potassium 2,5,8-tri(4'-pyridyl)-1,3,4,6,7,9-hexaazaphenalene) and ZnI_2 produced seven types of networks depending on the solvent systems (MeOH/additive solvent): $[\text{ZnI}(\text{TPHAP})] 3.5\text{CH}_3\text{OH}$ (**1**) (from MeOH/DMA), $[\text{ZnCl}_{0.5}\text{I}_{0.5}(\text{TPHAP})\text{H}_2\text{O}] 7\text{H}_2\text{O}$ (**2**) (from MeOH/DMA+water), $[\text{ZnI}(\text{TPHAP})] 3\text{PhOH} 2\text{CH}_3\text{OH}$ (**3**) (from MeOH/phenol (< 33%)), $[\text{ZnI}(\text{TPHAP})] 5\text{PhOH} 2.5\text{CH}_3\text{OH}$ (**4**) (from MeOH/phenol (> 50%)), $[\text{ZnI}(\text{TPHAP})] 2\text{PhNO}_2 6\text{CH}_3\text{OH}$ (from MeOH/nitrobenzene) (**5**), $[\text{ZnI}(\text{TPHAP})\text{CH}_3\text{OH}] 3\text{PhNH}_2$ (**6**) (from MeOH/aniline), and $[(\text{ZnI})_2(\text{TPHAP})(\text{HCON}(\text{CH}_3)_2)_3(\text{CH}_3\text{OH})_2]^+[(\text{ZnI})_2(\text{TPHAP})(\text{HCON}(\text{CH}_3)_2)]^- (\text{HCON}(\text{CH}_3)_2) 4\text{CH}_3\text{OH}$ (**7**) (from MeOH/DMF). All structures were characterized by single crystal X-ray structure determination. Each topology was analyzed by TOPOS. The structures were categorized into two- or three-periodic structure. The structural features of each network were explained by the weak intermolecular interactions between TPHAP^- and guest molecules. We demonstrated the multi-interactivity of TPHAP^- which can recognize the slight difference of weak intermolecular interactions.

Introduction

Coordination network is one of representative subjects of crystal engineering.¹ Network topology is based on the coordination geometry of metal ions and the shape of organic ligands. A combination of metal ions and organic ligands can form a number of unique networks.² Furthermore, weak intermolecular interactions like hydrogen bond and π - π interactions play a crucial role in networking.³ Even same components of metal ions and organic ligands can produce several kinds of networks depending on an energy landscape directed by experimental conditions, e.g. solvent, guest molecule, temperature, reaction speed, and so on.⁴ Although various topologies were reported, the number of porous networks composed of the same combination of metal ions and ligands is generally limited. To demonstrate the importance of intermolecular interactions in network formation, we focused on a hexaazaphenaleny (HAP) skeleton to introduce weak intermolecular interactions.⁵ We synthesized a multi-interactive ligand, potassium 2,5,8-tri(4'-pyridyl)-1,3,4,6,7,9-hexaazaphenalene (K^+TPHAP^-), which is sensitive to weak intermolecular interactions (Scheme 1).⁶ TPHAP^- has mainly three significant features: i) multi-dentate coordination sites, ii) a large aromatic plane, iii) six hydrogen bond acceptor sites.

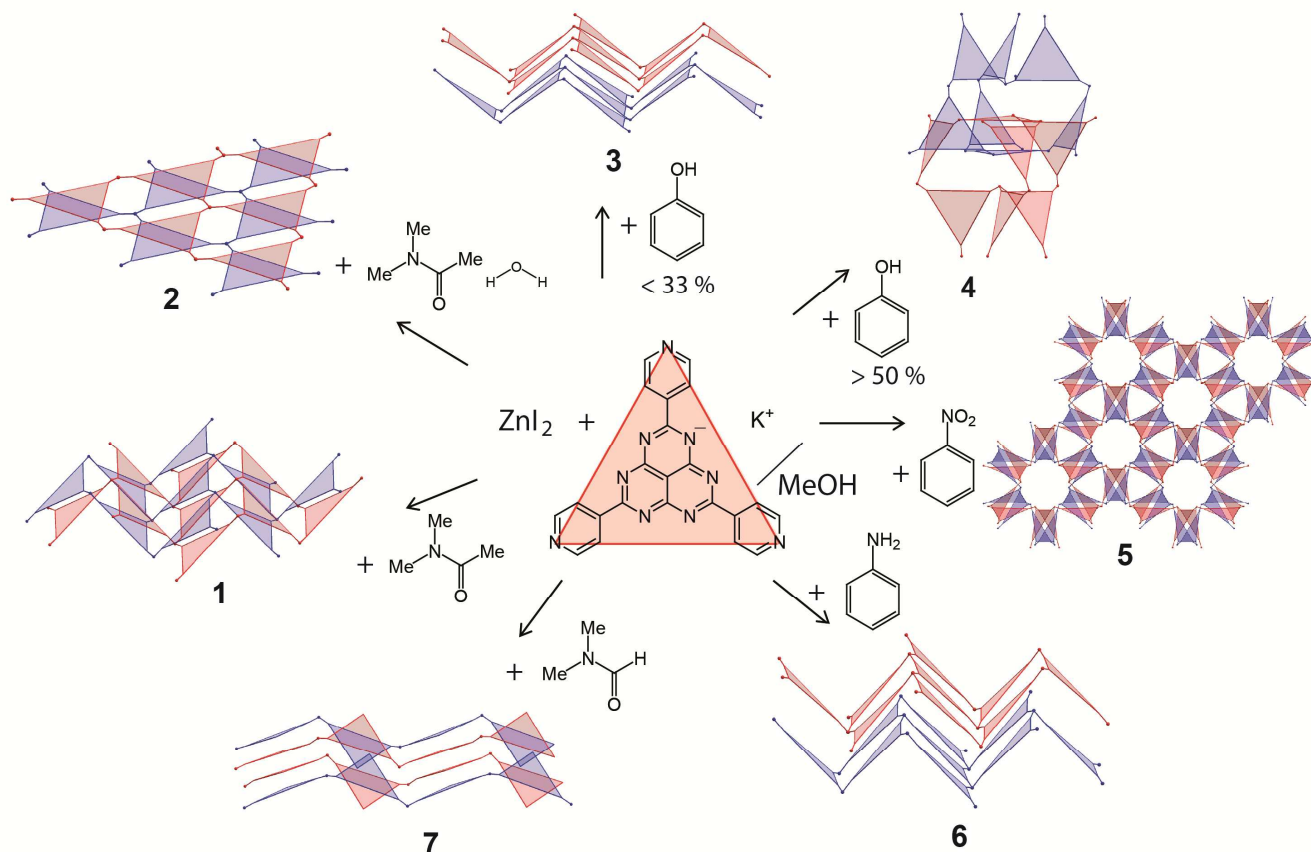


Scheme 1 The molecular structure of TPHAP^-

These interactive sites can induce weak intermolecular interactions during self-assembly. Therefore, this ligand can trap various kinetic states because weak intermolecular interactions deepen local potential energy minima.⁷ Indeed, the TPHAP^- ligand can form a variety of networks depending on the slightly different experimental conditions. We reported coordination networks composed of TPHAP^- and Co^{2+} and the dynamic structure transformation depending on temperature.⁶ In this study, we investigated solvent effects on networking. Solvent effects sometime make crystal engineering more difficult, especially in polymorph.⁸ A large number of polymorphs obtained from various solvents were reported. Here, we report seven kinds of coordination networks using the

same starting materials of K^+TPHAP^- and ZnI_2 in various solvents: $[ZnI(TPHAP)] 3.5CH_3OH$ (**1**), $[ZnCl_{0.5}I_{0.5}(TPHAP)H_2O] 7H_2O$ (**2**), $[ZnI(TPHAP)] 3PhOH 2CH_3OH$ (**3**), $[ZnI(TPHAP)] 5PhOH 2.5CH_3OH$ (**4**), $[ZnI(TPHAP)] 2PhNO_2 6CH_3OH$ (**5**), $[ZnI(TPHAP)CH_3OH] 3PhNH_2$ (**6**),

$[(ZnI)_2(TPHAP)(HCON(CH_3)_2)_3(CH_3OH)_2]^{+}[(ZnI)_2(TPHAP)(HCON(CH_3)_2)]^{-}$ ($HCON(CH_3)_2$) $4CH_3OH$ (**7**) (Scheme 2). This diversity of Zn^{2+} - $TPHAP^-$ coordination networks exemplifies the multi-interactivity of $TPHAP^-$ via weak intermolecular interaction.



Scheme 2 Diversity of Zn(TPHAP) network

Table 1 Experimental conditions and structural features

	Additive solvent ^a	Point symbol	Vertex symbol	RCSR	Type of network ^b	Coordination geometry	% of pore space against the unit cell volume ^c	Volume for a pore / Å ³
1	DMA, DMSO, 1,4-dioxane, THF	{6 ³ }	[6.6.6]	hcb	2-periodic undulated 6 ³ - hcb 2-fold interpenetrating with stacking ABABAB along [1,0,0]	Tetrahedral	29.3	848.3
2	DMA+H ₂ O	{6 ³ }	[6.6.6]	hcb	Single flat 6 ³ - hcb with stacking ABABAB along [0,0,1]	Trigonal bipyramidal	23.8	325.6
3	Phenol	{6 ³ }	[6.6.6]	hcb	Single undulated 6 ³ - hcb with stacking ABABAB along [0,1,0]	Tetrahedral	54.6	567.1
4	Phenol	{10 ³ }	[10 ₅ .10 ₅ .10 ₅]	srs	3-periodic 2-fold interpenetration of 10 ³ - srs net	Tetrahedral	63.2	1640.6
5	Nitrobenzene	{8 ³ }	[8.8.8 ₂]	etf	3-periodic 2-fold interpenetration of 8 ³ - etf net	Tetrahedral	66.4	1420.6, 2780.7
6	Aniline	{6 ³ }	[6.6.6]	hcb	Single undulated 6 ³ - hcb with stacking ABABAB along [1,0,0]	Pseudo-tetrahedral	47.4	463.9
7	DMF	{0}	-	-	1-D chain running all parallel to [1,0,1]	Tetrahedral & Octahedral	13.6	542.4

^a See experimental section. ^b Analyzed by TOPOS.¹⁰ ^c Calculated on 3.1. Mercury.

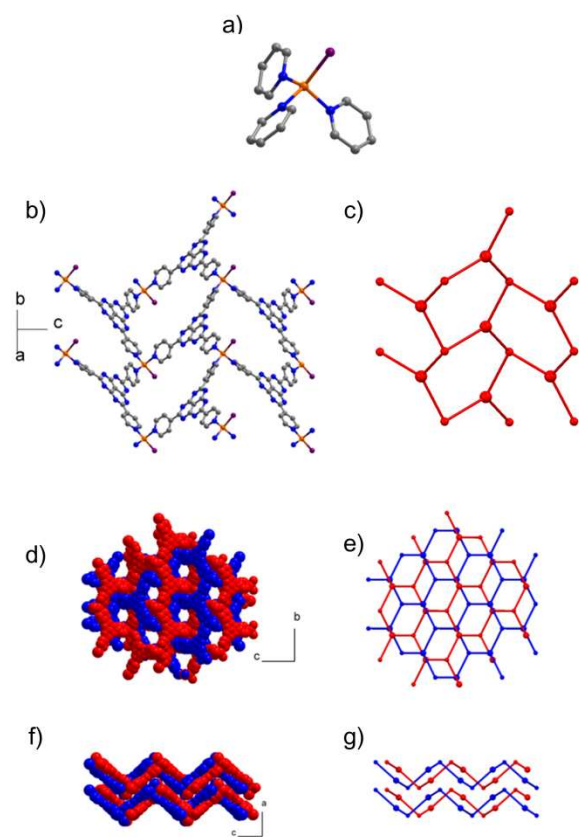


Fig.1 Crystal structure and schematic view of **1**. a) Zn^{2+} tetrahedral coordination environment by three tridentate TPHAP^- s and Γ^- . Orange, violet, blue, and gray spheres represent Zn, I, N and C atoms. H atoms are omitted for clarity. b) Zigzag sheet structure composed of $\text{ZnI}(\text{TPHAP})$. Zn^{2+} ion act as a trident junction. c) 3-c net schematic structure of zigzag sheet. d) Interpenetrating zigzag sheet structure viewed from the a axis, showing one-dimensional channels. e) Schematic view of interpenetrating zigzag sheet structure from top. f) Interpenetrating zigzag sheet structure viewed from the b axis, showing no space for guest-encapsulation between TPHAP^- s. g) Schematic view of interpenetrating zigzag sheet structure from side, showing stacking ABABAB.

Results

Syntheses and Characterization

The layering diffusion method of a methanol solution of ZnI_2 into a MeOH -guest solution of K^+TPHAP^- produced single crystals. Totally seven types of different network crystals were obtained depending on solvent and the mixing ratio (Table 1).^{9,10}

Crystal structure

1 $[\text{ZnI}(\text{TPHAP})] 3.5\text{CH}_3\text{OH}$

1 was obtained from methanol/additive solvent which has no hydrogen bond donor site such as DMA, DMSO, 1,4-dioxane and THF (Fig. 1). The network of **1** consists of TPHAP^- , Γ^- and Zn^{2+} . The Zn^{2+} centre has a tetrahedral geometry coordinated by three tridentate TPHAP^- s and Γ^- , forming zigzag sheet structure. Furthermore, two zigzag sheets interpenetrate each other. Because both of a ZnI^+ unit and a TPHAP^-

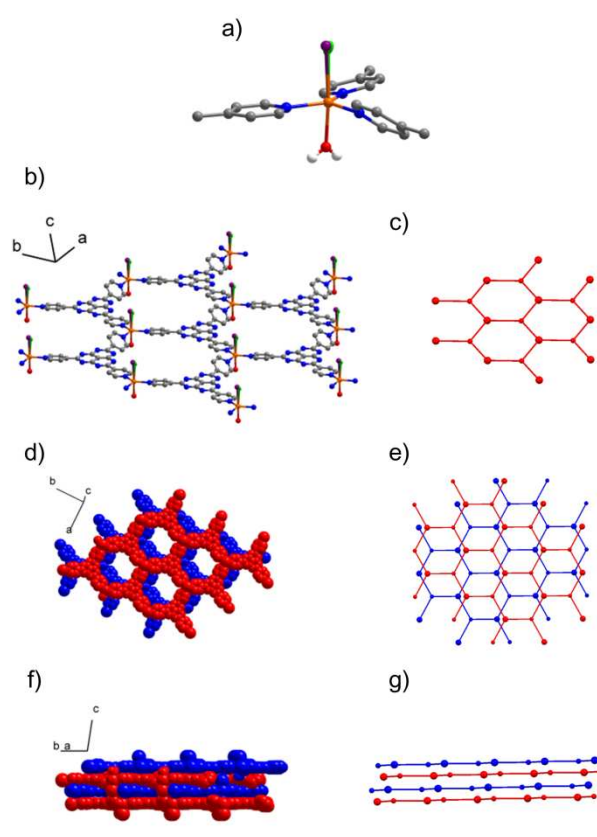


Fig.2 Crystal structure and schematic view of **2**. a) Zn^{2+} trigonal bipyramidal molecular geometry by three tridentate TPHAP^- s, water and Γ^- (or Cl^-). Colour codes are the same as those in Fig. 1 and red and green spheres represent O and Cl, respectively. b) Planar sheet structure composed of $\text{Zn}_{0.5}\text{Cl}_{0.5}(\text{TPHAP})\text{H}_2\text{O}$. Zn^{2+} ion acts as a trident junction. c) 3-c net schematic structure of planar sheet. d) Top view of planar sheet stacking structure, showing one-dimensional channel. e) Schematic view of planar sheet stacking structure from top. f) Side view of planar sheet stacking structure, showing no space for guest-encapsulation between TPHAP^- s. g) Schematic view of planar sheet stacking viewed from side, showing stacking ABABAB.

molecule can be regarded as a 3-connected node, **1** represents a uninodal 3-c net and TOPOS indicates that the zigzag sheet structure is 6^3-hcb (Fig. 1e). The interpenetrating networks stack each other via π - π interaction to form layers along the a axis (Fig. 1g) and 1D channels containing methanol. The interpenetrating structure **1** has a smaller void (27.4% against the unit cell volume) than do other networks which were obtained from aromatic solvent.

2 $[\text{ZnCl}_{0.5}\text{I}_{0.5}(\text{TPHAP})\text{H}_2\text{O}] 7\text{H}_2\text{O}$

2 was obtained from water/DMA/methanol (Fig. 2). The Zn^{2+} centre forms a five coordinate of a trigonal bipyramidal geometry composed of three tridentate TPHAP^- s, a water and Γ^- or Cl^- (Γ^- and Cl^- are disordered at a similar position and each occupancy factor was converged to 0.5 and 0.5, respectively) (Fig. 2a).¹¹ In a similar way to **1**, both a ZnI^+ unit and a TPHAP^- molecule act as a 3-connected node. Therefore, **2** represents a uninodal 3-c net, but the trigonal coordination of three TPHAP^- s forms a planar sheet 6^3-hcb structure which is

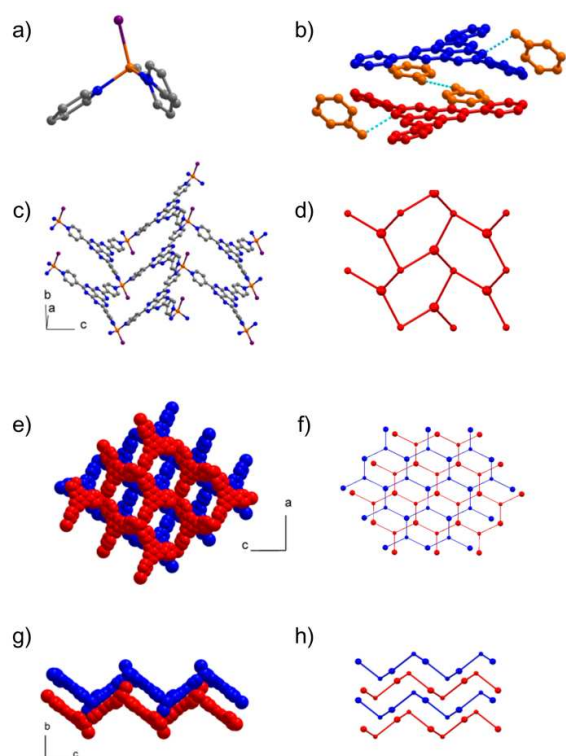


Fig. 3 Crystal structure and schematic view of **3**. a) Zn^{2+} tetrahedral coordination environment by three tridentate TPHAP⁻s and Γ^- in a similar way to **3**. b) Encapsulation of phenols (orange) between TPHAP⁻s (blue and red) via π - π interaction and a hydrogen bond. c) Zigzag sheet structure composed of Zn(TPHAP). Zn^{2+} ion acts as a trident junction. d) 3-c net schematic structure of zigzag sheet. e) Non-interpenetrating zigzag sheet stacking structure viewed from the *b* axis. f) Schematic view of non-interpenetrating zigzag sheet stacking structure from top. g) Non-interpenetrating zigzag sheet stacking structure viewed from the *a* axis. h) Schematic view of planar sheet stacking viewed from the side, showing stacking ABABAB.

different from a zigzag sheet structure in **1**. All planar sheets stack each other via π - π interaction along the *c* axis. Several waters locate in a pore and form a water cluster.

3 [ZnI(TPHAP)] 3PhOH 2CH₃OH

3 was obtained from phenol/methanol (phenol volumetric ratio < 33%) (Fig. 3). The network **3** is the non-interpenetrating version of **1** which is a zigzag sheet 6³-hcb structure. The zigzag sheets stack each other via π - π interaction along the *b* axis without interpenetration. Therefore, the void space (58.0%) is larger than that of **1**. One phenol is encapsulated in a void via π - π interaction with TPHAP⁻ forming a triple π stacking structure (TPHAP⁻/PhOH/TPHAP⁻). Another phenol forms a hydrogen bond to the nitrogen atom on the central TPHAP⁻ skeleton.

4 [ZnI(TPHAP)] 5PhOH 2.5CH₃OH

4 with the same component of ZnI(TPHAP) in **3** was obtained from methanol/phenol (phenol volumetric ratio > 50%) (Fig. 4). Although both a Zn atom and a TPHAP⁻ molecule act as 3-connected nodes, **4** has different interpenetrating 3D network. TOPOS indicates that **4** has 2-fold interpenetration of 10³-srs net. A phenol is sandwiched between TPHAP⁻s via π - π

interaction. An iodide locates above the TPHAP⁻, forming the iodine/TPHAP⁻/phenol/TPHAP⁻/iodine arrangement. The total void (68.0%) is larger than that of **2**. Four phenols form hydrogen bonds to nitrogen atoms on two central TPHAP⁻ skeletons. **4** has more hydrogen bonds than does **3**.

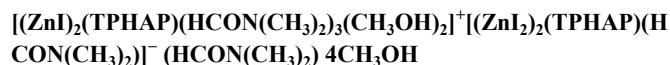
5 [ZnI(TPHAP)] 2PhNO₂ 6CH₃OH

Unexpected 3D network **5** was obtained from nitrobenzene/methanol (Fig. 5). The Zn^{2+} centre has a tetrahedral geometry coordinated by three tridentate TPHAP⁻s and Γ^- . The component of network and the uninodal 3-c net are the same as those of **1**, **3** and **4**. However, the network structure is different from those. TOPOS indicates that **5** has 2-fold interpenetration of 8³-etf net. This classification of network topology is the first example in the database of TOPOS&RCSR.^{9,12} The network **5** has two kinds of 1D channels along the *c* axis, so-called, biporous structure. Each channel is surrounded by different characteristic environments, halogen space (surrounded by iodine) and π space (surrounded by TPHAP⁻). Aromatic nitrobenzene prefers the π space via π - π interaction with TPHAP⁻. Differently from other solvent systems, nitrobenzene can form π -stacking dimer, therefore quadruple π -stacking structure consists of two TPHAP⁻ and two nitrobenzene (TPHAP⁻/nitrobenzene/nitrobenzene/TPHAP⁻). Thanks to the nitrobenzene dimer, this network has a large void (66.9%).

6 [ZnI(TPHAP)CH₃OH] 3PhNH₂

The combination of methanol/aniline produced the zigzag sheet structure [ZnI(TPHAP)CH₃OH] slightly different from **3** (Fig. 6). Although the Zn^{2+} centre has five coordinate by three TPHAP⁻s, Γ^- and a methanol, the network connectivity is the same, a uninodal 3-c net, as that of **3**. Therefore, the network is described as zigzag sheet 6³-hcb. However, because of methanol coordinating to Zn^{2+} , its dihedral angle between TPHAP⁻ planes slightly changed from 108.82(5) ° in **2** to 91.03(2) ° in **6** (Scheme 3). One aniline was encapsulated between TPHAP⁻s via π - π interaction.

7



7 was obtained from methanol/DMF (Fig. 7). Two kinds of 1D networks interpenetrate each other via π - π interaction. One 1D network consists of a bidentate TPHAP⁻ and ZnI_2 , in which the remaining pyridyl group and a carbonyl oxygen of DMF coordinate to ZnI_2 , forming a negatively charged network, $[(\text{ZnI}_2)_2(\text{TPHAP})(\text{HCON}(\text{CH}_3)_2)]^-$. The other 1D network also consists of a bidentate TPHAP⁻ and ZnI_2 , in which, however, the remaining pyridyl group of TPHAP⁻, three carbonyl oxygen of DMF and two methanol molecules coordinate to Zn^{2+} , forming positively charged network $[(\text{ZnI})_2(\text{TPHAP})(\text{HCON}(\text{CH}_3)_2)_3(\text{CH}_3\text{OH})_2]^+$. To the best of our knowledge, this network is the first hybrid open framework composed of alternatively arrayed positively- and negatively-charged 1D chains.

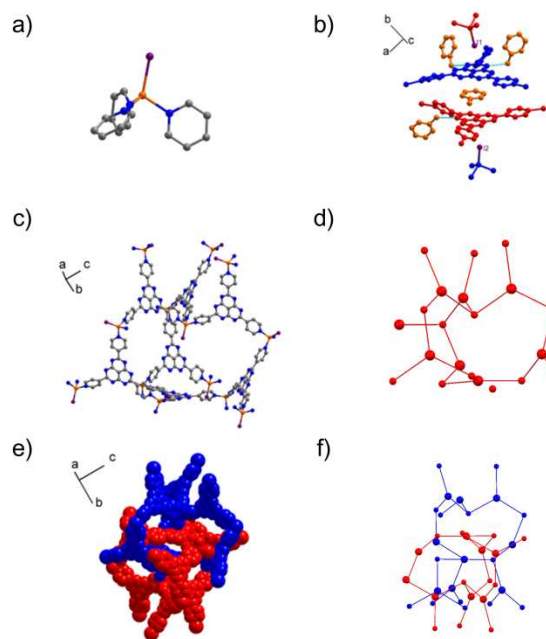


Fig. 4 Crystal structure and schematic view of **4**. a) Zn^{2+} tetrahedral coordination environment by three tridentate TPHAP's and I^- in a similar way to **1** and **3**. b) Encapsulation of phenols (orange) between TPHAP's (blue and red) via π - π interaction and hydrogen bond. Iodide locates above the TPHAP $^-$. c) 3D network composed of $\text{ZnI}(\text{TPHAP})$. Zn^{2+} ion acts as a trident junction. d) 3-c net schematic structure of 3D network. e) Interpenetrating 3D network. f) Schematic view of 2-fold interpenetrating 3D network.

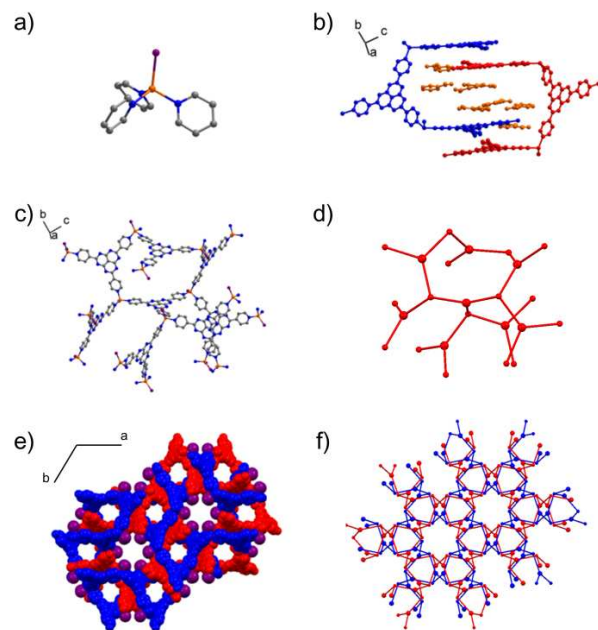


Fig. 5 Crystal structure and schematic view of **5**. a) Zn^{2+} tetrahedral coordination environment by three tridentate TPHAP's and I^- in a similar way to **1**, **3** and **4**. Colour codes are the same as those in Fig. 1. b) Encapsulation of nitrobenzene dimer (orange) between TPHAP's (blue and red) via π - π interaction. c) 3D network composed of $\text{ZnI}(\text{TPHAP})$. d) 3-c net schematic structure of 3D network. e) Interpenetrating biporous 3D network, showing two kinds of 1D channels which are surrounded by π planes and iodine atoms (violet). f) Schematic view of interpenetrating biporous 3D network viewed from the top.

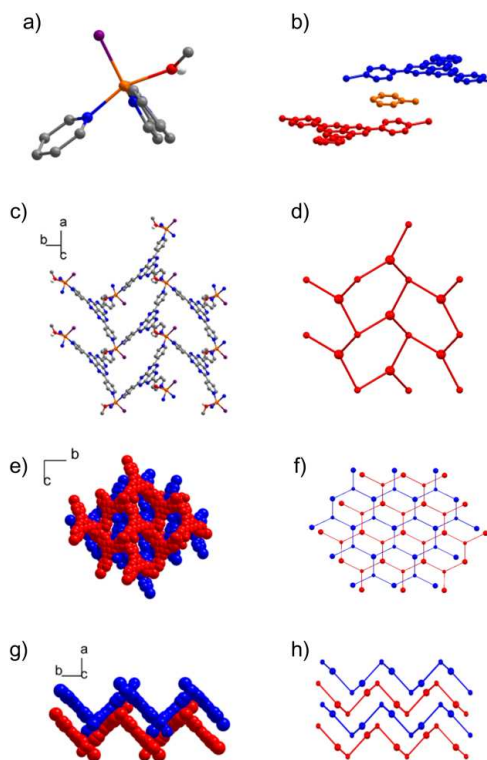


Fig. 6 Crystal structure and schematic view of **6**. a) Zn^{2+} pseudo-tetrahedral coordination environment by three tridentate TPHAP's, I^- and methanol. Colour codes are the same as those in Fig. 2. b) Encapsulation of anilines (orange) between TPHAP's via π - π interaction. c) Zigzag sheet structure composed of $\text{ZnI}(\text{TPHAP})\text{CH}_3\text{OH}$. d) 3-c net schematic structure of zigzag sheet. e) Zigzag sheet stacking structure without interpenetration viewed from the a axis. f) Schematic view of non-interpenetrating zigzag sheet stacking structure from top. g) Non-interpenetrating zigzag sheet stacking structure viewed from the c axis, showing spaces which can encapsulate anilines between TPHAP's. h) Schematic view of planar sheet stacking viewed from the side, showing stacking ABABAB.

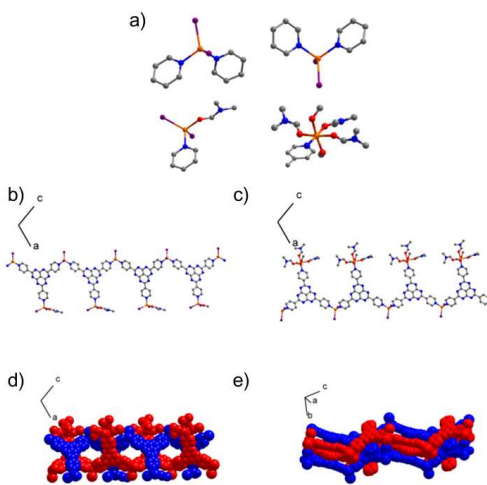


Fig. 7 Crystal structure of **7**. a) Four types of Zn^{2+} coordination environment. Upper left: tetrahedral $\text{ZnI}_2(\text{TPHAP})_2$, upper right: tetrahedral $\text{ZnI}_2(\text{TPHAP})_2$, lower left: tetrahedral $\text{ZnI}_2(\text{TPHAP})(\text{DMF})$ and lower right: octahedral $\text{Zn}(\text{TPHAP})(\text{DMF})_3(\text{MeOH})_2$. Colour codes are the same as those in Fig. 2. b) An anionic 1D chain of $[(\text{ZnI}_2)_2(\text{TPHAP})(\text{HCON}(\text{CH}_3))]^-$. c) A cationic 1D chain of $[(\text{ZnI})_2(\text{TPHAP})(\text{HCON}(\text{CH}_3)_2)_3(\text{CH}_3\text{OH})_2]^+$. d) Top view of alternative zigzag chain structure. e) Side view of alternative zigzag chain structure, showing no space for guest encapsulation between TPHAP's.

Table 2 Crystal data and experimental conditions

	1	2	3	4	5	6	7
Empirical formula	C _{25.5} H ₂₆ IN ₉ O _{3.5} Zn	C ₂₂ H ₂₈ Cl _{0.5} I _{0.5} N ₉ O ₈ Zn	C ₄₂ H ₃₈ IN ₉ O ₈ Zn	C _{54.5} H ₅₂ IN ₉ O _{7.5} Zn	C ₄₀ H ₄₆ IN ₁₁ O ₁₀ Zn	C ₄₁ H ₃₇ IN ₁₂ OZn	C ₆₅ H ₈₃ I ₆ N ₂₅ O ₁₁ Zn ₄
Formula weight	706.82	693.08	941.08	1145.32	1033.15	906.10	2385.42
Temperature / K	100(2)	100(2)	100(2)	100(2)	85(2)	100(2)	100(2)
Wavelength / Å	0.71073	0.71073	0.68898	0.71073	0.68900	0.68899	0.75002
crystal system	Orthorhombic	Monoclinic	Monoclinic	Orthorhombic	Trigonal	Monoclinic	Monoclinic
Space group	<i>Pna</i> 2 ₁	<i>C2/c</i>	<i>P2₁/n</i>	<i>P2₁2₁2₁</i>	<i>R-3c</i>	<i>P2₁/n</i>	<i>P2₁/n</i>
<i>a</i> / Å	18.006(1)	26.47(2)	15.4187(2)	21.500(11)	44.006(1)	15.1138(1)	23.1344(2)
<i>b</i> / Å	15.3229(9)	15.79(1)	12.4644(2)	21.500(11)	44.006(1)	18.5709(1)	14.7104(1)
<i>c</i> / Å	20.969(1)	13.591(9)	21.6037(3)	22.454(12)	28.267(1)	15.6792(1)	26.8906(3)
<i>α</i> / °	90	90	90	90	90	90	90
<i>β</i> / °	90	105.64(2)	90.208(1)	90	90	117.2124(2)	110.4115(3)
<i>γ</i> / °	90	90	90	90	120	90	90
Volume / Å ³	5785.4(6)	5468(6)	4151.9(1)	10379(9)	47406(2)	3913.78(4)	8576.7(1)
Z	8	8	4	8	36	4	4
Reflection collected / unique	24289 / 10434	36789 / 5553	66389 / 9607	38905 / 11792	140618 / 12797	83134 / 11903	139867 / 19129
<i>R</i> (int)	0.0390	0.0592	0.0409	0.1084	0.0785	0.0464	0.0571
Final <i>R</i> indices	<i>R</i> ₁ = 0.0931	<i>R</i> ₁ = 0.0598	<i>R</i> ₁ = 0.1162	<i>R</i> ₁ = 0.0890	<i>R</i> ₁ = 0.1240	<i>R</i> ₁ = 0.0657	<i>R</i> ₁ = 0.0663
[<i>I</i> > 2σ(<i>I</i>)]	<i>wR</i> ₂ = 0.2607	<i>wR</i> ₂ = 0.1471	<i>wR</i> ₂ = 0.3266	<i>wR</i> ₂ = 0.2329	<i>wR</i> ₂ = 0.3556	<i>wR</i> ₂ = 0.1794	<i>wR</i> ₂ = 0.1760
<i>R</i> indices (all data)	<i>R</i> ₁ = 0.1367	<i>R</i> ₁ = 0.0913	<i>R</i> ₁ = 0.1326	<i>R</i> ₁ = 0.1357	<i>R</i> ₁ = 0.1610	<i>R</i> ₁ = 0.0752	<i>R</i> ₁ = 0.0831
	<i>wR</i> ₂ = 0.2969	<i>wR</i> ₂ = 0.1635	<i>wR</i> ₂ = 0.3389	<i>wR</i> ₂ = 0.2519	<i>wR</i> ₂ = 0.3849	<i>wR</i> ₂ = 0.1873	<i>wR</i> ₂ = 0.1878
$\Delta\rho_{max}, \Delta\rho_{min}/e \text{ \AA}^{-3}$	1.873, -1.502	0.987, -0.617	2.098, -1.653	1.504, -0.711	2.123, -1.414	1.246, -2.852	1.363, -2.622

Discussion

Effect of solvent on network topology and coordination environment

We obtained four kinds of topology (interpenetrating 6³-hcb, non-interpenetrating 6³-hcb, interpenetrating 10³-srs, and interpenetrating 8³-etf) except for 7 (Table 1). All networks are composed of the same component, ZnI(TPHAP), in which both ZnI⁺ and TPHAP⁻ act as 3-connected nodes. Previously, Kawano, Fujita and co-workers reported 62 networks by using TPT (2,4,6-tris(4-pyridyl)-1,3,5-triazine) ligand and they were categorized into four topology (10³-srs, 10³-ths, 4².6, and 6³-hcb).^{9,12} The topology consist of one kind of node, 3-connected TPT ligand, in which TPT ligand does not act as a C₃ symmetrical node because each TPT ligand is connected by lower symmetry of ZnI₂. Therefore, all TPT networks do not have the strong isotropic property.¹³ To form strong isotropic property, a higher symmetrical node is required. On the other hand, ZnI(TPHAP) networks consist of two kinds of C₃ symmetry nodes: TPHAP⁻ and ZnI⁺. Therefore, ZnI(TPHAP) may produce stronger isotropic property networks than ZnI₂(TPT). Further, we explain topological mechanism on the basis of symmetry of node and the weak intermolecular interactions between TPHAP⁻ and guest molecules.

1) 2-periodic 6³-hcb structures

1, **2**, **3**, and **6** are similar 2-periodic 6³-hcb structures. It is worth noting that, in **1**, **2**, **3**, and **6** networks, π-π interaction dominates intermolecular interactions within TPHAP⁻ molecules, forming a dimer of TPHAP⁻s. Especially, **1**, **3**, and **6** have the same 6³-hcb zigzag sheet, however each stacking structure is different. While the 6³-hcb zigzag sheets in **1** interpenetrate each other, those in **3** and **6** are stacked without

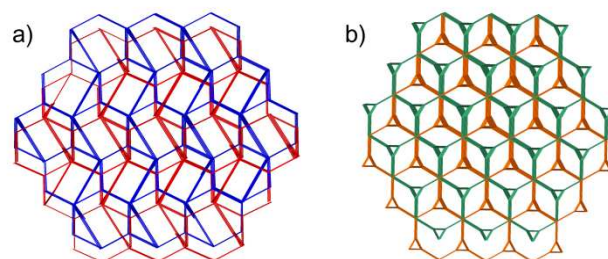


Fig.8 a) Schematic view of **4**, showing interpenetrating 10³-srs network. b) Schematic view of strong isotropic interpenetrating 10³-srs network composed of C_{3h} symmetry node.

interpenetration.¹⁴ Because **1** was obtained from the non-aromatic solvent system (methanol/DMA, DMSO, 1,4-dioxane or THF), π-π interaction may dominate intermolecular interactions within only TPHAP⁻ molecules, followed by interpenetrating network formation with a 27.4% void. On the other hand, because **3** and **6** were obtained from aromatic solvent (methanol/phenol and methanol/aniline, respectively), the solvent molecules were encapsulated in a void via π-π interaction with TPHAP⁻, leading to non-interpenetrating network. Therefore, the voids in **3** and **6** (54.6% and 47.4%, respectively) are larger than that of **1**.

2) Interpenetrating 10³-srs structure

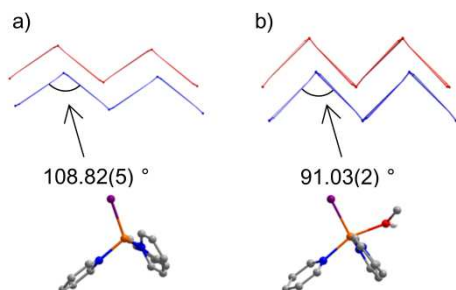
3-periodic interpenetrating 10³-srs structure, **4**, was obtained from the same solvent system as in **3** (PhOH/MeOH). The different ratio of phenol (volumetric ratio < 33% or > 50%) generated totally different networks, 6³-hcb (**3**) and 10³-srs (**4**), respectively. Among uninodal 3-c nets, hcb and srs are well-known networks with 2445 and 307 examples in TOPOS&RCSR database.¹² As Sunada mentioned, 10³-srs nets possesses strong symmetry.¹³ Especially, a pair of

interpenetrating 10^3 -srs nets is similar to so-called gyroid structure with 84 examples.¹⁵ Among them, only 6 examples are the strong isotropic gyroid structures (Fig. 8b), which consist of organic ligands and metal connector as C_3 symmetry of nodes.¹⁶ In this study, **4** forms gyroid structure thanks to C_3 symmetry of both nodes, Zn^{2+} and $TPHAP^-$ (Fig. 8a). The 10^3 -srs network **4** obtained from phenol-rich solution (> 50% volumetric ratio) has a large void occupied by solvent through hydrogen bond and π - π interaction, in which phenol prefers hydrogen bond to π - π interaction, probably preventing $TPHAP^-$ dimer formation. Thanks to multi-interactive and highly symmetrical C_3 $TPHAP^-$ and metal connector, we successfully constructed the strong isotropic gyroid structure, **4**.

3) Interpenetrating 8^3 -etf structure

5 forms 3-periodic 2-fold interpenetrating 8^3 -etf network composed of Zn^{2+} and $TPHAP^-$. Network **5** has a larger void between $TPHAP^-$ dimers. $TPHAP^-$ and nitrobenzene form quadruple π -stacking structure ($TPHAP^-/nitrobenzene/nitrobenzene/TPHAP^-$). Among all, thanks to nitrobenzene double layer, only **5** has a pore window large enough for guest molecules to enter.

Zn^{2+} ions in **2**, **6** and **7** have different coordination geometry. Network **2** and **7** were obtained from the solvent systems containing water and DMF which can coordinate to metal ions. Therefore, it is not surprising that they provided unique coordination geometry. However, in the case of **6**, even though aniline did not coordinate to Zn^{2+} ions, the coordination geometry changed slightly from tetrahedral to pseudo-tetrahedral by additional methanol coordination thanks to the flexibility of coordination mode of Zn ions (Scheme 3).



Scheme 3 Dihedral angle between $TPHAP^-$ planes and trident junction part of Zn^{2+} : a) in **3** and b) in **6**.

Networking mechanism through cation-assisted dimerization

From the structural point of view, except for **4**, it is noteworthy that a dimer of $TPHAP^-$ s can be regarded as one unit. This result indicates that in solution $TPHAP^-$ s form a dimer, and that the dimerization helps networking (scheme 4). To check the species in solution state, we measured cold-spray ionization mass spectra (ESI-MS).¹⁷ A peak of $[K(TPHAP)_2]^-$ ($m/z=843.219$) species was observed in CSI-MS (Fig. 9). The crystal structure of K^+TPHAP^- suggests that this species forms

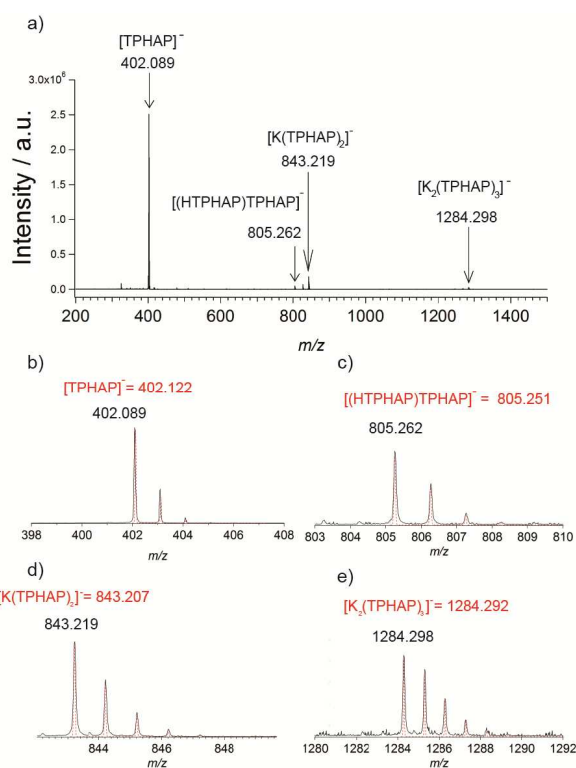
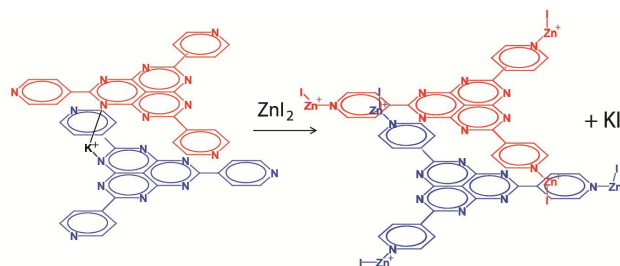


Fig. 9 a) CSI-MS spectrum of K^+TPHAP^- in methanol (negative mode). b) Magnified experimental (black) and simulated (red) spectra from $TPHAP^-$ for the range $m/z = 398-408$. c) Magnified experimental and simulated spectra from $[(HTPHAP)TPHAP]^-$ for the range $m/z = 803-810$. d) Magnified experimental and simulated spectra from $[K(TPHAP)_2]^-$ for the range $m/z = 842-850$. e) Magnified experimental and simulated spectra from $[K_2(TPHAP)_3]^-$ for the range $m/z = 1280-1292$.



Scheme 4 Proposed networking mechanism

a dimer not only with K^+ ion bridging but also via π - π interaction. This result supports our assumption that dimerization assisted by K^+ may help ligand exchange during networking. Even using smaller ionic cation salt such as Li^+TPHAP^- and Na^+TPHAP^- , ESI-MS showed dimerization in solution, e.g. $[Li(TPHAP)_2]^-$ ($m/z=810.252$) and $[Na(TPHAP)_2]^-$ ($m/z=827.240$). Indeed, using those salts, we obtained **5**. Furthermore, as a control experiment, we failed to form **5** using an organic cation salt, $[(C_6H_5)_4P]^+TPHAP^-$, which cannot assist dimerization. So far we also have never succeeded in networking with the same crystallization method using H^+TPHAP^- . Even though dimer $[(H^+TPHAP^-)TPHAP]^-$ ($m/z=805.262$) was detected by CSI-MS, it is likely that the strength of dimerization is weaker than the dimer assisted by

metal ion $[M(\text{TPHAP})_2]^-$ ($M = \text{Li}^+, \text{Na}^+, \text{and } \text{K}^+$). Still other factors can be considered for the reasons that the TPHAP neutral form cannot produce any network yet. However, this cation-assisted dimerization can be an important factor for networking.

Conclusions

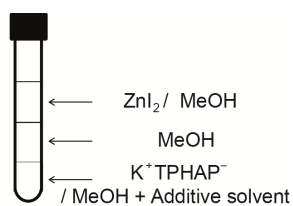
We showed the diversity of multi-interactivity of TPHAP^- via weak intermolecular interactions in coordination network formation. TPHAP^- and Zn^{2+} produced seven types of networks depending on the nature of solvent. Among them, **1**, **3**, **4** and **5** consist of the same component, $\text{ZnI}(\text{TPHAP})$. Especially, although **3** and **4** were obtained from the same solvent system (PhOH/MeOH), different networks were formed due to the different solvent ratio. This fact indicates that a slight difference in experimental conditions makes a big difference in networking thanks to multi-interactivity of TPHAP^- to weak intermolecular interactions. Furthermore, this extreme multi-interactivity can generate two kinds of pores surrounded by π plane and iodine in **5**, which can be expected a unique selectivity for guest exchange. In conclusion, we demonstrated that TPHAP^- can be an excellent probe for weak intermolecular interactions and can form various networks depending on coexisting molecules. This interactive ligand can be useful for trapping kinetic state networks.

Experimental

General procedures

All reagents were purchased from commercial sources and used without further purification unless otherwise noted. The following reagents were used for crystallization: 99.5% dimethylacetamide (DMA), 99.8% dimethylsulfoxide (DMSO), 99.0% phenol, 99.0% nitrobenzene, 99.5% dimethylformamide (DMF), (SAMCHUN); 99.5% aniline (Sigma Aldrich). 99.5% Methanol (SAMCHUN) was dried over 4 Å molecular sieves. K^+TPHAP^- was prepared by following the procedure described in Ref. 6.

Elemental analyses were performed by Vario MICRO Cube (Elementar) at Technical support center in Pohang University of Science and Technology. FTIR-ATR (attenuated total reflection) spectra were recorded on a Varian 670-IR FT-IR spectrometer ($650\text{--}4000\text{ cm}^{-1}$). The samples for elemental analysis and FTIR-ATR were dried at room temperature under vacuum.



Scheme 5 Crystallization set up

Synthesis

1 $[\text{ZnI}(\text{TPHAP})] \cdot 3.5\text{CH}_3\text{OH}$

The single crystals were grown from a triple-layered solution consisting of a 2 ml methanol solution of ZnI_2 (59.2 mM) as the top layer, 2 ml methanol as the middle layer, and 2 ml DMA/methanol solution (1.5 ml DMA + 0.5 ml methanol) of K^+TPHAP^- (9.5 mM) as the bottom layer at $14\text{ }^\circ\text{C}$. After a few days, pale yellow crystals were grown. Anal. Calcd for $\text{C}_{22}\text{H}_{24}\text{N}_9\text{O}_6\text{IZn}$ ($= (\text{C}_{22}\text{H}_{12}\text{N}_9)(\text{ZnI})(\text{H}_2\text{O})_6$) (%): C, 37.60; H, 3.44; N, 17.94 %. Found: C, 37.69; H, 3.37; N, 17.81. IR (ATR, $\nu_{\text{max}}/\text{cm}^{-1}$): 3200s, 1595vs, 1560s, 1480w, 1420m, 1380w, 1330m, 1300s, 1180w, 1080w, 1055w, 1030w, 935w, 845w, 755w, 740w, 690w.

2 $[\text{ZnCl}_{0.5}\text{I}_{0.5}(\text{TPHAP})\text{H}_2\text{O}] \cdot 7\text{H}_2\text{O}$

The single crystals were grown from a triple-layered solution consisting of 2 ml methanol solution of ZnI_2 (59.2 mM) as the top layer, 2 ml methanol/water mixture (1.9 ml methanol + 0.1 ml water) as the middle layer, and 2 ml DMA/methanol solution (1.5 ml DMA + 0.5 ml methanol) of K^+TPHAP^- (9.5 mM) as the bottom layer at $14\text{ }^\circ\text{C}$. After a few days, pale yellow crystals were grown. Anal. Calcd for $\text{C}_{24}\text{H}_{26}\text{Cl}_{0.5}\text{I}_{0.5}\text{N}_9\text{O}_5\text{Zn}$ ($= (\text{C}_{22}\text{H}_{12}\text{N}_9)(\text{ZnCl}_{0.5}\text{I}_{0.5})(\text{CH}_4\text{O})_2(\text{H}_2\text{O})_3$) (%): C, 43.21; H, 3.93; N, 18.90 %. Found: C, 43.04; H, 3.65; N, 18.88. IR (ATR, $\nu_{\text{max}}/\text{cm}^{-1}$): 3360s, 1590vs, 1560s, 1505s, 1480w, 1420m, 1375w, 1325m, 1300s, 1210vw, 1180w, 1075w, 1050w, 1030w, 1015w, 930w, 840w, 755w, 740w, 695w, 680w.

3 $[\text{ZnI}(\text{TPHAP})] \cdot 3\text{PhOH} \cdot 2\text{CH}_3\text{OH}$

The single crystals were grown from a triple-layered solution consisting of 2 ml methanol solution of ZnI_2 (59.2 mM) as the top layer, 2 ml methanol/phenol mixture (1.5 ml methanol + 0.5 ml phenol) as the middle layer, and 2 ml phenol/methanol solution (1.5 ml phenol + 0.5 ml methanol) of K^+TPHAP^- (9.5 mM) as the bottom layer at $14\text{ }^\circ\text{C}$. After a few days, pale yellow crystals were grown. Anal. Calcd for $\text{C}_{40}\text{H}_{31.4}\text{IN}_9\text{O}_{3.7}\text{Zn}$ ($= (\text{C}_{22}\text{H}_{12}\text{N}_9)(\text{ZnI})(\text{C}_6\text{H}_6\text{O})_3(\text{H}_2\text{O})_{0.7}$) (%): C, 54.00; H, 3.56; N, 14.17 %. Found: C, 54.40; H, 3.48; N, 13.79. IR (ATR, $\nu_{\text{max}}/\text{cm}^{-1}$): 3200s, 1590vs, 1560s, 1500w, 1480w, 1420m, 1380w, 1325w, 1300m, 1240w, 1170w, 1080w, 1055w, 1030w, 935w, 845w, 810vw, 755w, 740w, 690w.

4 $[\text{ZnI}(\text{TPHAP})] \cdot 5\text{PhOH} \cdot 2.5\text{CH}_3\text{OH}$

The single crystals were grown from a triple-layered solution consisting of 2 ml methanol solution of ZnI_2 (59.2 mM) as the top layer, 2 ml methanol/phenol mixture (0.5 ml methanol + 1.5 ml phenol) as the middle layer, and 2 ml phenol/methanol solution (1.5 ml phenol + 0.5 ml methanol) of K^+TPHAP^- (9.5 mM) as the bottom layer at $14\text{ }^\circ\text{C}$. After a few days, pale yellow crystals were grown. Anal. Calcd for $\text{C}_{22}\text{H}_{24}\text{IN}_9\text{O}_6\text{Zn}$ ($= (\text{C}_{22}\text{H}_{12}\text{N}_9)(\text{ZnI})(\text{C}_6\text{H}_6\text{O})_5(\text{CH}_4\text{O})_{2.5}$) (%): C, 37.60; H, 3.44; N, 17.94. Found: C, 37.69; H, 3.37; N, 17.81. IR (ATR, $\nu_{\text{max}}/\text{cm}^{-1}$): 3200s, 1595vs, 1560s, 1500w, 1480w, 1420m, 1380w, 1325m,

1300s, 1175w, 1080w, 1055w, 1030w, 935w, 845w, 810vw, 755w, 735w, 690w.

5 [ZnI(TPHAP)] 2PhNO₂ 6CH₃OH

The single crystals were grown from a triple-layered solution consisting of 2 ml methanol solution of ZnI₂ (59.2 mM) as the top layer, 2 ml methanol as the middle layer, and 2 ml nitrobenzene /methanol solution (1.5 ml nitrobenzene + 0.5 ml methanol) of K⁺TPHAP⁻ (9.5 mM) as the bottom layer at 14 °C. After a few days, pale yellow crystals were grown. Anal. Calcd for C_{40.9}H₄₂Cl_{0.2}IK_{0.2}N_{11.4}O_{9.3}Zn (= (C₂₂H₁₂N₉)(ZnI)(C₆H₅NO₂)_{2.4}(CH₄O)_{4.5}(KCl)_{0.2}) (%): C, 46.82; H, 4.03; N, 15.22. Found: C, 46.59; H, 3.74; N, 14.96. IR (ATR, ν_{max} /cm⁻¹): 3200s, 1595vs, 1560s, 1520w, 1480w, 1420m, 1380w, 1345vw, 1325m, 1300s, 1175w, 1080w, 1055w, 1030w, 935w, 845w, 810vw, 755w, 735w, 690w.

6 [ZnI(TPHAP)CH₃OH] 3PhNH₂

The single crystals were grown from a triple-layered solution consisting of 2 ml methanol solution of ZnI₂ (59.2 mM) as the top layer, 2 ml methanol as the middle layer, and 2 ml aniline /methanol solution (1.5 ml aniline + 0.5 ml methanol) of K⁺TPHAP⁻ (9.5 mM) as the bottom layer at 14 °C. After a few days, brown crystals were grown. Anal. Calcd for C₂₈H₂₅Cl_{0.5}IK_{0.5}N₁₀O₃Zn (= (C₂₂H₁₂N₉)(ZnI)(C₆NH₇)(H₂O)₃(KCl)_{0.5}) (%): C, 43.16; H, 3.23; N, 17.98. Found: C, 43.03; H, 2.87; N, 17.68. IR (ATR, ν_{max} /cm⁻¹): 3200s, 1590vs, 1560s, 1520w, 1495w, 1480w, 1420m, 1380w, 1345vw, 1325m, 1300s, 1175w, 1080w, 1055w, 1030w, 930w, 845w, 810vw, 755w, 740w, 690w.

7

[(ZnI)₂(TPHAP)(HCON(CH₃)₂)₃(CH₃OH)₂]⁺[(ZnI)₂(TPHAP)(HCON(CH₃)₂)₃]⁻ 4CH₃OH

The single crystals were grown from a triple-layered solution consisting of 2 ml methanol solution of ZnI₂ (59.2 mM) as the top layer, 2 ml methanol as the middle layer, and 2 ml DMF /methanol solution (1.5 ml DMF + 0.5 ml methanol) of K⁺TPHAP⁻ (9.5 mM) as the bottom layer at 14 °C. After a few days, pale yellow crystals were grown. Anal. Calcd for C₅₈H₆₀I₆N₂₂O₆Zn₄ (= [(TPHAP)(ZnI)(DMF)₃(MeOH)₂][(TPHAP)(ZnI)₂(DMF)₃]) (%): C, 31.89; H, 2.77; N, 14.11. Found: C, 31.87; H, 3.09; N, 14.37. IR (ATR, ν_{max} /cm⁻¹): 3330s, 1650vw, 1595vs, 1560s, 1480w, 1420m, 1380w, 1325m, 1300s, 1175w, 1080w, 1055w, 1030w, 930w, 845w, 810vw, 755w, 740w, 690w.

Single Crystal X-ray Structure Determination

The diffraction data for **1**, **2** and **4** were recorded with a Bruker APEX-II/CCD QUAZAR diffractometer equipped with a focusing mirror (MoK α radiation, λ = 0.71073 Å). Empirical absorption corrections were applied with the data using the program SADABS.

The diffraction data for **5** was recorded with a RIGAKU/MSC Mercury CCD X-ray diffractometer with a synchrotron radiation (λ = 0.6889 Å) at PF-AR (NW2A beamline) of the

High Energy Accelerator Research Organization (KEK). The diffraction images were processed by using HKL2000.¹⁸ Absorption correction was performed with the program PLATON.¹⁹

The diffraction data for **3**, **6** and **7** were recorded with an ADSC Q210 CCD area detector with a synchrotron radiation at 2D beamline in Pohang Accelerator Laboratory (PAL). The diffraction images were processed by using HKL3000.¹⁸ Absorption correction was performed with the program PLATON.

Each structure was solved by the direct methods using SHELXS-97²⁰ and refined by the full-matrix least-squares method on F² using SHELXL-97.²¹

Cold spray ionization mass spectra

Cold spray ionization mass spectrometry (CSI-MS) measurements were carried out with a microTOF time-of-flight mass spectrometer (Bruker Daltonics). A CSI unit was attached to the ESI-MS measurement system for the CSI-MS measurements. Negative mode was employed for all measurements (capillary voltage: 3.5 kV, capillary exit-skimmer potential difference: 30 V). CSI-MS spectrum was obtained by direct infusion of methanol solutions of K⁺TPHAP⁻ by using a syringe pump with a rate of 750 $\mu\text{L}\cdot\text{h}^{-1}$. The desolvation temperature was set to 30 °C.

Acknowledgements

This research was supported by the BK21 Plus (10Z2013000023) and Basic Research (Project No. 2011-0009930) through the National Research Foundation of Korea (NRF) grant funded by the Ministry of Education, Science and Technology (MEST). X-ray diffraction study with synchrotron radiation was performed at PF-AR (NW2A beamline) of the High Energy Accelerator Research Organization (KEK) (Proposal No. 2012G017) and at the Pohang Accelerator Laboratory (Beamline 2D) supported by POSTECH (Proposal No. 2012-3rd-2D-003). T.Y. thanks the Ministry of Education, Science, and Technology of Japan (MEXT) for financial support through the Joint Research and Dispatch Program of the Gifu University Young Researchers Education Center for Innovation.

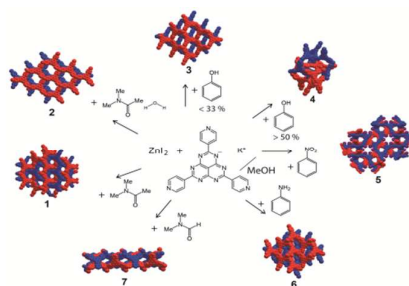
Notes and references

- a* Division of Advanced Materials Science, Pohang University of Science and Technology (POSTECH), Pohang 790-784, Korea.; Fax: (+82)-54-279-8739; Tel: (+82)-54-279-8740; E-mail: mkawano@postech.ac.kr
b Department of Chemistry, Faculty of Engineering, Gifu University, Yanagido 1-1, Gifu, 501-1193, Japan
c Department of Applied Chemistry, Chubu University, Kasugai, Aichi 487-8501, Japan.
d Department of Chemistry, Graduate School of Science, Osaka University, Machikaneyama 1-1, Toyonaka, Osaka 560-0043, Japan.

† Electronic Supplementary Information (ESI) available: [CCDC 944048-944054 contain the supplementary crystallographic data for this paper. These data can be obtained free of charge from The Cambridge Crystallographic Data

Centre via www.ccdc.cam.ac.uk/data_request/cif. See DOI: 10.1039/b000000x/

- 1 G. R. Desiraju, J. J. Vittal and A. Ramanan, *Crystal Engineering: A Textbook*, World Scientific, Singapore, 2011.
- 2 (a) S. R. Batten and R. Robson, *Angew. Chem. Int. Ed.*, 1998, **37**, 1460. (b) M. Eddaoudi, D. B. Moler, H. Li, B. Chen, T. M. Reineke, M. O. Keffe and O. M. Yaghi, *Acc. Chem. Res.*, 2001, **34**, 319. (c) O. R. Evans and W. Lin, *Acc. Chem. Res.*, 2002, **38**, 511. (d) S. Kitagawa, R. Kitaura and S. Noro, *Angew. Chem., Int. Ed.*, 2004, **43**, 2334. (e) M. Kawano and M. Fujita, *Coord. Chem. Rev.*, 2007, **251**, 2592. (f) G. Ferey, *Chem. Soc. Rev.*, 2008, **37**, 191. (g) J. J. Perry, J. A. Perman and M. J. Zaworotko, *Chem. Soc. Rev.*, 2009, **38**, 1400. (h) O. K. Farha and J. T. Hupp, *Acc. Chem. Res.*, 2010, **43**, 1166. (i) M. O. Keffe and O. M. Yaghi, *Chem. Rev.*, 2012, **112**, 675.
- 3 (a) J. S. Seo, D. Whang, H. Lee, S. I. Jun, J. Oh, Y. J. Jeon and K. Kim, *Nature*, 2000, **404**, 982. (b) R. Kitaura, K. Fujimoto, S. Noro, M. Kondo and S. Kitagawa, *Angew. Chem. Int. Ed.*, 2002, **41**, 133. (c) D. M. Shin, I. S. Lee and Y. K. Chung, *Inorg. Chem.*, 2003, **42**, 8838. (d) R. Custelcean and M. G. Gorbunova, *J. Am. Chem. Soc.*, 2005, **127**, 16362. (e) S. Hasegawa, S. Horike, R. Matsuda, S. Furukawa, K. Mochizuki, Y. Kinoshita and S. Kitagawa, *J. Am. Chem. Soc.*, 2007, **129**, 2607. (f) J. M. Roberts, B. M. Fini, A. A. Sarjeant, O. K. Farha, J. T. Hupp and K. A. Scheidt, *J. Am. Chem. Soc.*, 2012, **134**, 3334.
- 4 (a) K. Biradha and M. Fujita, *Angew. Chem., Int. Ed.*, 2002, **41**, 3392. (b) O. Ohmori, M. Kawano and M. Fujita, *Angew. Chem., Int. Ed.*, 2009, **44**, 1962. (c) K. Ohara, J. Marti-Rujas, T. Haneda, M. Kawano, D. Hashizume, F. Izumi and M. Fujita, *J. Am. Chem. Soc.*, 2009, **131**, 3860. (d) J. Marti-Rujas and M. Kawano, *Acc. Chem. Res.*, 2013, **46**, 493. (e) H. Kitagawa, H. Ohtsu and M. Kawano, *Angew. Chem., Int. Ed.*, 2013, **125**, 12621.
- 5 (a) S. Suzuki, Y. Morita, K. Fukui, K. Sato, D. Shiomi, T. Takui and K. Nakasuji, *Inorg. Chem.*, 2005, **44**, 8197; (b) S. Suzuki, K. Fukui, A. Fuyuhira, K. Sato, T. Takui, K. Nakasuji and Y. Morita, *Org. Lett.*, 2010, **12**, 5036.
- 6 Y. Yakiyama, A. Ueda, Y. Morita and M. Kawano, *Chem. Commun.*, 2012, **48**, 10651.
- 7 M. Chaplin, *Nat. Rev. Mol. Cell Biol.*, 2006, **7**, 861.
- 8 (a) G. R. Desiraju, *Angew. Chem. Int. Ed.*, 2007, **46**, 8342. (b) C.-P. Li and M. Du, *Chem. Commun.*, 2011, **47**, 5958. (c) S. Chen, I. A. Guzei and L. Yu, *J. Am. Chem. Soc.*, 2005, **127**, 9881. (d) V. López-Mejías, J. W. Kampf and A. J. Matzger, *J. Am. Chem. Soc.*, 2012, **134**, 9872.
- 9 (a) V. A. Blatov, *Cryst. Rev.* 2004, **10**, 249. (b) V. A. Blatov, *IUCr CompComm Newsletter*, 2006, **7**, 4.; <http://www.topos.ssu.samara.ru>.
- 10 Terminology followed the recommendation by V. A. Blatov, D. M. Proserpio and M.O'Keeffe. V. A. Blatov, D. M. Proserpio and M.O'Keeffe, *CrystEngComm*, 2010, **12**, 44.
- 11 Cl⁻ comes from a small amount of KCl contained as impurity which was not removed by purification of K⁺TPHAP⁻. Because of high solubility of KCl in water, KCl affected formation of compound **2** obtained from DMA/methanol/water.
- 12 (a) O. Delgado-Friedrichs, M.O'Keeffe and O. M. Yaghi, *Acta Crystallogr., Sect. A: Found. Crystallogr.*, 2003, **59**, 22. (b) V. A. Blatov, L. Carlucci, G. Ciani and D. M. Proserpio, *CrystEngComm*, 2004, **6**, 377. (c) I. A. Baburin, V. A. Blatov, L. Carlucci, G. Ciani and D. M. Proserpio, *J. Solid State Chem.*, 2005, **178**, 2452. (d) M.O'Keeffe, M.A. Peskov, S. J. Ramsden and O. M. Yaghi, *Acc. Chem. Res.* 2008, **41**, 1782.; <http://rcsr.anu.edu.au>. (e) E. V. Alexandrov, V. A. Blatov, A. V. Kochetkov and D. M. Proserpio, *CrystEngComm*, 2011, **13**, 3947.
- 13 (a) T. Sunada, *Not. Am. Math. Soc.*, 2008, **55**, 208. (b) S. T. Hyde, M.O'Keeffe and D. M. Proserpio, *Angew. Chem. Int. Ed.*, 2008, **47**, 7996.
- 14 (a) L. Carlucci, G. Ciani and D. M. Proserpio, *Coord. Chem. Rev.*, 2003, **246**, 247. (b) D. M. Proserpio, *Nat. Chem.*, 2010, **2**, 435.
- 15 (a) S. T. Hyde, S. Andersson, B. Ericsson and K. Larsson, *Z. Kristallogr.*, 1984, **168**, 213. (b) A. H. Schoen, NASA Technical Note, TN D-5541, 1970.
- 16 (a) R. Custelcean and P. Remy, *Cryst. Growth. Des.*, 2009, **9**, 1985. (b) D. Li, W. J. Shi and L. Hou, *Inorg. Chem.*, 2005, **44**, 3907.
- 17 K. Yamaguchi, *J. Mass. Spectrom.*, 2003, **38**, 473
- 18 Z. Otwinowski and W. Minor, *Methods Enzymol.*, 1997, **276A**, 307.
- 19 A. L. Spek, *Acta Crystallogr., Sect D*, 2009, **65**, 148.
- 20 G. M. Sheldrick, University of Göttingen, Germany, **1996**.
- 21 G. M. Sheldrick, Acta Crystallographica Section A, **2008**, A64, 112.



The Diversity of Zn(II) Coordination Networks Composed of Multi-Interactive Ligand TPHAP⁻ via Weak Intermolecular Interaction

Tatsuhiro Kojima, Tomofumi Yamada, Yumi Yakiyama, Eri Ishikawa, Yasushi Morita, Masahiro Ebihara, and Masaki Kawano

Seven types of different Zn(TPHAP) coordination networks were prepared thanks to the excellent multi-interactivity of TPHAP for weak intermolecular interaction.